Inner-shell photoemission from the iodine atom in CH_3I

D. W. Lindle, P. H. Kobrin,* C. M. Truesdale,† T. A. Ferrett, P. A. Heimann, H. G. Kerkhoff,‡ U. Becker,‡ and D. A. Shirley

Materials and Molecular Research Division, Lawrence Berkeley Laboratory, Berkeley, California 94720 and Department of Chemistry, University of California, Berkeley, California 94720

(Received 23 December 1983)

The first photoemission measurements of the I $4d$ and I "$4p$" subshells in methyl iodide are presented. Cross sections and angular-distribution asymmetry parameters were measured from threshold to 300 eV photon energy for the I $4d$ level (to 440 eV for the asymmetry parameter), and from 175 to 300 eV for the I "$4p$" level. The I $4d$ results exhibited atomiclike behavior throughout this energy range, mimicking the behavior of the Xe $4d$ subshell. Theoretical calculations for the Xe $4d$ subshell agree very well with the I $4d$ asymmetry-parameter results, indicating that the I $4d$ subshell is localized on the iodine atom in CH_3I. Nearer to threshold, the spin-orbit final states, $4d_{5/2}$ and $4d_{3/2}$, were resolved and exhibited nonstatistical intensity ratios mainly due to a kinetic energy effect. The I "$4p$" asymmetry-parameter results were found to be essentially identical to the asymmetry-parameter results for the I $4d$ subshell at the same photon energies, suggesting strong interchannel coupling. This result is discussed with respect to collective effects in the iodine N shell.

I. INTRODUCTION

Recent photoelectron-spectroscopy (PES) studies[1–8] of Xe have highlighted both one-electron and multielectron effects that are important in describing photoionization in the N and O shells of Xe above the $4d$ threshold. Elucidation of these effects has been accomplished by comparison of the experimental results to progressively more detailed theoretical calculations.[9–20] One result has been to identify Xe and other elements with similar Z as especially good systems for exhibiting some of these effects. The present photon-energy-dependent PES study of the iodine atom in CH_3I adds considerably to the available experimental measurements for elements near Xe in the Periodic Table.

For photon energies immediately above the $4d$ ionization threshold [Xe (Refs. 7 and 8) or I], the photoelectron spectrum is dominated by features associated with $4d$-vacancy states. It is known[7] that photoemission from the Xe $4d$ subshell can be described accurately by considering a series of single-electron effects that appear in the $4d \rightarrow \epsilon f$ continuum channel; a Coulomb phase shift occurs near threshold, followed at somewhat higher energy by a shape resonance resulting from the trapping of the outgoing photoelectron by a centrifugal barrier, and finally at still higher energy, the $4d \rightarrow \epsilon f$ dipole matrix element experiences a change in sign and causes a Cooper minimum. Experimentally, pronounced changes corresponding to these phenomena have been seen in the subshell cross section,[2] the spin-orbit branching ratio,[4,5] and the angular distribution of Xe $4d$ photoelectrons.[3,7] To the extent that the iodine atom in a molecule such as CH_3I exhibits atomiclike behavior, the present measurements yield information about the Z dependence of the one-electron effects peculiar to $4d \rightarrow \epsilon f$ transitions. The present results indicate that the inner subshells of I in CH_3I are atomiclike. The I $4d$ subshell shows behavior remarkably similar to Xe $4d$, with some small systematic variations. These results are discussed in Sec. III A.

Multielectron effects generally become more important for the less intense (smaller cross section) features in photoelectron spectra. This is especially true for the "$4p$" subshells of the elements in the series Te to Ba.[1,16] Quotation marks are used here because the final states that have binding energies in the vicinity of the $4p$ thresholds can be described adequately only in terms of collective effects;[16] hence designation as a $4p$ final state is inappropriate. In Xe for example, only one major discrete peak is observed in this energy range along with continuumlike structure,[1] contrary to the one-electron-model prediction of two peaks corresponding to the $4p_{3/2}$ and $4p_{1/2}$ ionic states. The prominent peak has been attributed primarily to the $4d^8 4f$ configuration, and the remaining structure is explained in terms of the near degeneracy of $4p$-vacancy states with $4d^8 nl$ singly ionized and $4d^8$ doubly ionized states.[16] As this near degeneracy is enhanced (or removed) by observing different Z elements, significant changes in the "$4p$" spectra are seen.[1] For I, the discrete structure is less intense than in Xe, and the identification of the single observed peak as a $4p$-hole state is even more questionable. The cross section and angular distribution of the I "$4p$" peak as functions of photon energy are presented here for the first time (note that similar measurements have not yet been made for Xe "$4p$"). The asymmetry-parameter results are nearly identical to the I $4d$ results at the same photon energies. Though interpretation of these results is not straightforward, the assignment of the final state as $4d^8 4f$ is consistent with the results discussed in Sec. III B. A brief description of the experiment is given in Sec. II. Conclusions are discussed in Sec. IV.

II. EXPERIMENTAL

Photons from beam line III-1 at the Stanford Synchrotron Radiation Laboratory were used to ionize an effusive

jet of CH_3I molecules. Photoelectron spectra were recorded simultaneously at two angles, 0° and 54.7°, with respect to the polarization vector of the incident photon beam by measuring the elecron flight times to identical channel-plate detectors. The apparatus and the time-of-flight (TOF) detectors have been described elsewhere.[21] Briefly, the ultrahigh vacuum monochromator was protected by a 1500-Å-thick Al window from the $\sim 10^{-5}$ Torr in the experimental chamber. The photon beam was focused to the center of the chamber to intersect the gas jet at the interaction region defined by the apertures of the TOF detectors. The relative photon flux was monitored by a sodium salicylate scintillator and an optical photomultiplier tube (RCA 8850). The gas pressure was recorded with a capacitance manometer.

Yang's theorem[22] defines the differential cross section, $d\sigma/d\Omega$, for photoionization of a randomly oriented sample by linearly polarized radiation as

$$\frac{d\sigma(h\nu)}{d\Omega} = \frac{\sigma(h\nu)}{4\pi}[1+\beta(h\nu)P_2(\cos\theta)] , \quad (1)$$

where θ is the angle between the momentum vector of the ejected electron and the polarization vector of the incident photon, $P_2(\cos\theta)$ is the second Legendre polynomial, and $\sigma(h\nu)$ and $\beta(h\nu)$ are the cross section and the angular-distribution asymmetry parameter, respectively, for the photoionization process under study. The dependence of σ and β on the photon energy $h\nu$ has been included here explicitly, but will be omitted throughout the remainder of this paper. Equation (1) implies the assumption that only electric dipole transitions are important. Also implicit in Eq. (1) is that the photon source is 100% linearly polarized. The polarization of the photons from BL III-1 has been estimated to be 98%,[8] and it has been demonstrated previously that the precise value of the polarization is unimportant for our work (as long as it is greater than 70%), because of the calibration procedure described in Ref. 23.

The TOF technique is well suited to the measurement of photoelectron spectra of gases because of its high signal-to-noise ratio and its ability to collect nearly all electron energies simultaneously. Simultaneous measurement of the relative intensity of photoelectrons at two angles yields values of β that are independent of changes in the photon flux and gas pressure. To normalize our β measurements, known values of β for Ne $2p$ and $2s$ lines[24] were measured as a function of kinetic energy. This procedure is described in detail in Refs. 8 and 23. It is important to note that this procedure greatly reduces the effects of systematic errors in our measurements. We estimate systematic errors in β to be ± 0.10 or less. At certain photon-energy settings of the monochromator, a component of second-order radiation (i.e., an energy of $2h\nu$) was sufficiently large to produce additional peaks in our spectra, primarily second-order peaks of I $4d$ photoelectrons. Because the β measurements are independent of the photon flux, we were able to use these spectra to extend our β_{4d} results to higher photon energies.

Spectra taken with the 54.7° detector, for which $P_2(\cos\theta)$ vanishes, yield branching-ratio data directly, and cross-section data after correction for photon-flux and gas-pressure variations. The transmission of this analyzer was determined by measuring the known cross sections of the Ne L shell.[24] The contribution to the photon-flux measurement of the second-order light component also was determined by measuring the Ne L-shell cross sections, and a correction was made to the CH_3I cross-section results where needed.

III. RESULTS AND DISCUSSION

A representative TOF photoelectron spectrum of CH_3I at a photon energy of 64 eV is shown in Fig. 1. The predominance in this spectrum of features associated with I $4d$ ionization is apparent. The Auger peaks ($N_{4,5}VV$) result from the decay of the $4d$-vacancy states. Both Auger features receive contributions from many decay channels, and no attempt is made here to assign any of these Auger transitions. The following subsections treat in turn each subshell from which we were able to detect photoelectrons; I $4d$ in Sec. III A and I "$4p$" in Sec. III B.

A. I 4d subshell

Cross-section and asymmetry-parameter results for the I $4d$ subshell are shown in Figs. 2 and 3. These data are for the unresolved I $4d$ peak. Measurements in which the spin-orbit components, $4d_{5/2}$ and $4d_{3/2}$, are resolved at low kinetic energies are presented in Fig. 4. The binding energies of the $4d_{5/2}$ and $4d_{3/2}$ states are 56.7 and 58.3 eV, respectively.[25] The I $4d$ cross section has been scaled to the absolute photoabsorption measurement of O'Sullivan[25] at the maximum in the cross section. The peak value in the absorption cross section is approximately 17 Mb. As mentioned in Sec. II, the asymmetry-parameter results have been augmented by additional measurements with second-order light (see Fig. 1). The points obtained in this way are shown as open circles in Fig. 3.

Interpretation of the results for the I $4d$ subshell benefits from the previous measurements[2–5,7,8] and calculations[9–13,17,19,20] for the Xe $4d$ subshell. The I $4d$ cross section shows two important effects. At 85–90 eV, the

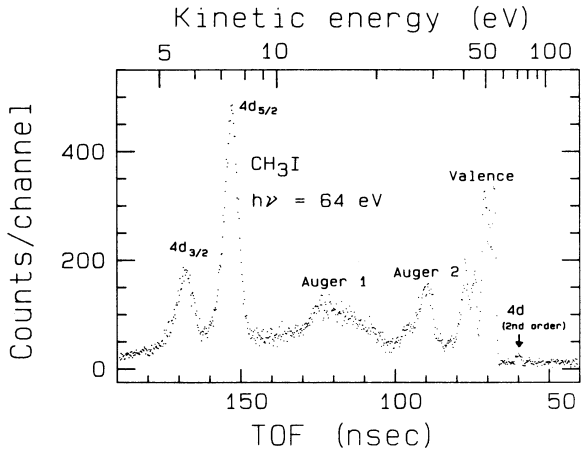

FIG. 1. Time-of-flight (TOF) spectrum of CH_3I at 64 eV photon energy taken with the 54.7° analyzer.

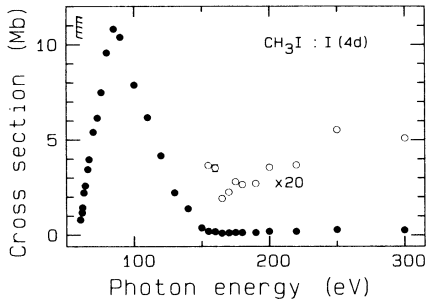

FIG. 2. Partial cross section of the I $4d$ subshell in CH_3I, scaled at 85 eV to the absorption measurement of O'Sullivan, Ref. 25. These data represent the sum of the cross sections for the spin-orbit components, $4d_{5/2}$ and $4d_{3/2}$, with an average binding energy of 57.5 eV. The photon resolution for the measurements in this work is a constant 1.3 Å full width at half maximum.

cross section reaches a maximum which can be attributed to a centrifugal-barrier shape-resonance effect in the $4d \rightarrow \epsilon f$ outgoing channel.[26] The position of the maximum agrees with the absorption measurement of O'Sullivan. The second effect occurs at 165—170 eV photon energy and can be assigned to a Cooper minimum[27] in the same $4d \rightarrow \epsilon f$ channel. Both of these phenomena in the I $4d$ subshell occur at the same photoelectron energy (± 5 eV) as in the Xe $4d$ case.[28–33] This concordance for the Cooper minima is based on comparison of the asymmetry-parameter data[7] because no measurements of the partial cross section at the Xe $4d$ Cooper minimum are available.

For $d \rightarrow \epsilon f$ transitions, the shape resonance is most pronounced for the elements in the Periodic Table centered around Xe (Ref. 26) because the $4f$ wave function has a high degree of continuum character in this sequence of atoms, so that virtual excitation to this orbital contributes significantly to the photoionization process.[34] This is apparently a general phenomenon. For the particular case of I $4d \rightarrow \epsilon f$, we are interested in the implications for the Z dependence of $4d$ cross sections.

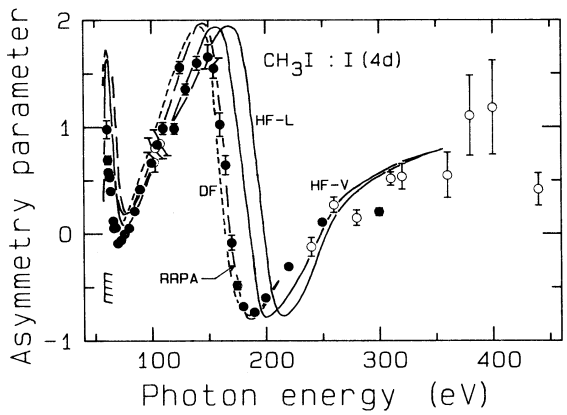

FIG. 3. Angular-distribution asymmetry parameter of the I $4d$ subshell in CH_3I. The data are weighted averages of the asymmetry parameters for the $4d_{5/2}$ and $4d_{3/2}$ final states. Solid and open circles represent data taken with first-order and second-order light, respectively. Theoretical calculations for the Xe $4d$ subshell shifted to coincide with the I $4d$ threshold; solid curves are Hartree-Fock length (HF-L) and velocity (HF-V) by Kennedy and Manson, Ref. 12; short-dashed curve is Dirac-Fock (DF) by Ong and Manson, Ref. 19; and long-dashed curve is relativistic random-phase approximation (RRPA) by Huang *et al.*, Ref. 20.

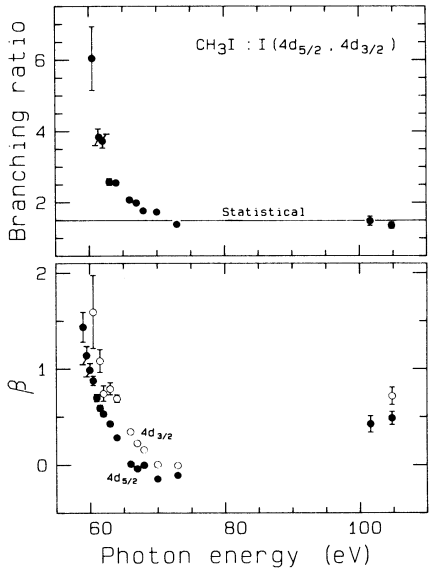

FIG. 4. Branching ratio (top) and asymmetry parameters (bottom) for the spin-orbit components, $4d_{5/2}$ and $4d_{3/2}$. The point at 101.6 eV in the bottom panel represents β for both final states.

Compared to Xe, the centrifugal barrier in I is somewhat higher (Z is lower), which should cause the cross section to peak at a higher kinetic energy than in Xe. Absorption measurements for the atomic species in the series Te,[35] I,[25,36–39] Xe,[28,29,31–33] and Cs (Refs. 37 and 40—42) (or molecules containing these atoms) imply a decrease of the kinetic energy of about 5 eV per series member for the shape-resonance maximum (approximately 40, 35, 30, and 25 eV, respectively). A photoemission measurement[2] of the Xe $4d$ cross section was consistent with the absorption result, but could not confirm it because of the scarcity of data points. Likewise, the present measurement and another using electron energy-loss spectroscopy[43] are consistent with the photoabsorption peak measured for CH_3I (Ref. 25) (32 eV above threshold) and I_2 (Ref. 35) (34 eV above threshold). However, our result also is consistent with the kinetic energy of the maximum in the Xe absorption[28,29,31] (30 eV) to within experimental error. We note the 2-eV difference between the peaks of the CH_3I and I_2 absorption results and suggest that it is due to molecular effects.

From a wave function overlap argument presented in Ref. 36, a second result of the higher barrier in I would be to reduce the $4d$ cross-section maximum compared to Xe. Unfortunately, experimental uncertainties in the present results and the previous measurements[2,36] preclude a quantitative determination.

A definite minimum is observed in the I $4d$ cross section which falls to a value of ~ 0.1 Mb at 165—170 eV photon energy, then increases by a factor of 2 at higher

energy. This minimum, which we interpret as a Cooper minimum arising from a sign change in the $4d \rightarrow \epsilon f$ matrix element, occurs at the same kinetic energy (± 5 eV) as the Cooper minimum in the Xe $4d$ subshell, as determined by comparison of the asymmetry-parameter results.[7] No other observations of Cooper minima in $4d$ subshell cross sections are available for further comparison.

The I $4d$ asymmetry-parameter results shown in Fig. 3 also are affected strongly by the shape-resonance and Cooper-minimum phenomena. The trapping of the outgoing photoelectron by the centrifugal barrier and the consequent phase shift are interpreted as causing the initial decrease in the measured $4d$ asymmetry. Because this happens before the barrier is overcome, the minimum in β_{4d} occurs at 15—20 eV lower kinetic energy than the maximum in the $4d$ cross section, or at approximately 70 eV photon energy.

Using the Cooper-Zare formula[44] for β in LS coupling, β_{4d} is predicted to be 0.1 at the Cooper minimum if spin-orbit and multielectron effects are neglected.[45] This value for β_{4d} is reached at a photon energy between 165 and 170 eV, in complete agreement with the minimum in the cross-section results.

The theoretical curves[12,19,20] in Fig. 3 represent calculations for the Xe $4d$ subshell that have been shifted 11 eV to lower energy for comparison with the I $4d$ results at the same kinetic energy. A detailed comparison of these curves to experiment for Xe has been given in Ref. 7. Overall, the similarity between the I $4d$ and Xe $4d$ results (experimental and theoretical) is remarkable, especially in the region of the Cooper minimum which is predicted best by the relativistic random-phase approximation[20] (RRPA) and Dirac-Fock[19] (DF) calculations. At lower energies, around 70 and 150 eV, differences between the I $4d$ results and the Xe $4d$ predictions are more apparent. This observation can be understood in the light of the differences between the shape resonances in Xe and I described above. Compared to the experimental Xe $4d$ results, we note a general tendency for I β_{4d} to be less than Xe β_{4d} by 0.2—0.3 at all energies, a result for which we have no explanation. Near threshold, no experimental evidence for the predicted initial increase in I β_{4d} is seen, in agreement with a similar finding from the Xe $4d$ results.[7]

One additional observation concerning the β_{4d} results pertains to the two points at 120 and 125 eV. Both of these points deviate significantly (by 0.3 or more) from a smooth curve connecting the remainder of the data. Because of the proximity of the I "$4p$" threshold at approximately 129 eV, we tentatively explain this behavior as autoionization of Rydberg states leading to this threshold. Clearly more experimental work with a finer mesh of points would be needed to confirm this conjecture.

At the lowest photon energies used in this work, the spin-orbit components of the I $4d$ peak were resolved (see Fig. 1). The $4d_{5/2}$-to-$4d_{3/2}$ intensity ratio is shown in Fig. 4. It starts at 6 at 60.5 eV and quickly drops to the statistical value of 1.5. This behavior is satisfactorily explained by a kinetic energy effect; at a given photon energy, the $4d_{5/2}$ peak has 1.6-eV-higher kinetic energy than the $4d_{3/2}$ peak, and thus is further along in its sharp increase in cross section caused by the shape resonance (see Fig. 2). The asymmetry parameters of the individual components are shown in the bottom of Fig. 4. They follow the same trend as the unresolved β_{4d} in Fig. 3. The differences between $\beta_{5/2}$ and $\beta_{3/2}$ are also explained by the kinetic energy effect.

An additional peak in the photoelectron spectra with a binding energy of 72(1) eV appeared at photon energies from 110 to 130 eV. This peak can be attributed to a correlation satellite(s) of the I $4d$ main line. It probably corresponds to final states with a $4d$ vacancy and a valence electron promoted from a nonbonding orbital localized on the I atom ($E_{3/2}$ or $E_{1/2}$) to a higher-lying antibonding valence orbital. The intensity of the satellite relative to the I $4d$ line is 15(4)% in this energy range. It appears strongly at these photon energies probably because it experiences the same shape-resonance effect as the I $4d$ cross section.

B. I "$4p$" Subshell

Svensson *et al.*[1] recorded Al $K\alpha$ photoelectron spectra of the series of elements Te to Ba in the regions of their respective $4p$ binding energies. Rather than finding two peaks ($4p_{3/2}$ and $4p_{1/2}$) corresponding to single-electron transitions to the final state, each of these elements showed distinct multielectron behavior to varying degrees; Te showing the largest effect, Ba the least. Wendin and Ohno[16] explained the situation for Xe in terms of strong many-electron effects that prevent the existence of an isolated $4p_{3/2}$- or $4p_{1/2}$-hole state, but require that a "$4p$" vacancy actually appears primarily as the Xe^+ $4d^8 4f$ state. This strong coupling results from the near degeneracy of a single $4p$ hole and a double vacancy with two $4d$ holes. A similar description is based on the onset of energy-allowed $N_{2,3}N_{4,5}N_{4,5}$ super-Coster-Kronig decay in the range of Z from 52 (Te) to 56 (Ba).[16]

Because the TOF detectors record photoelectrons over a wide range of energies simultaneously, we obtained several spectra of the I "$4p$" region of CH_3I while making the measurements on the I $4d$ subshell. The "$4p$" spectra looked very similar to that of Svensson *et al.*, and our measured binding energy of 129(1) eV agrees with theirs. The "$4p$" cross-section and asymmetry-parmeter results for photon energies from 175 to 300 eV are shown in Fig. 5. These values were determined by considering only the area under the single prominent ($4d^8 4f$) peak and by excluding as much as possible the broad continuumlike structure at higher binding energy (see Fig. 5 of Ref. 1 for a spectrum of CH_3I in this region). We interpret the data in Fig. 5 as primarily representing the $4d^8 4f$ final state.

The I "$4p$" cross-section data in the top of Fig. 5 were scaled to the previously scaled I $4d$ cross section. The intensity of the $4d^8 4f$ peak accounts for only 25—50% of the total intensity in the "$4p$" binding-energy region. The remainder is contained in the broad continuum. Taking this extra intensity into account, the total I "$4p$" cross section is approximately equal to the I $4d$ cross section in this photon-energy range.

The I "$4p$" asymmetry-parameter results (Fig. 5) start

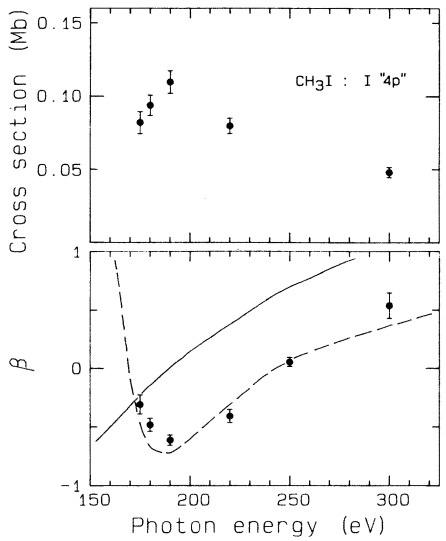

FIG. 5. Partial cross section (top) and asymmetry parameter (bottom) for I "$4p$" photoelectrons from CH_3I [129(1) eV binding energy]. The curves in the bottom panel represent HF-V calculations of Kennedy and Manson (solid), Ref. 12, and a smooth curve (dashed) drawn through the β_{4d} results in Fig. 3.

at -0.3 at 175 eV, drop to a minimum of -0.6 at 190 eV and reach 0.5 by 300 eV. Included in Fig. 5 is one curve representing a Hartree-Fock velocity (HF-V) calculation[12] of Xe β_{4p}, shifted in energy to coincide with the I "$4p$" threshold, and a second derived from a smooth curve through the I β_{4d} data in Fig. 3. The HF-V curve, which predicts the behavior of β_{4p} in a single-electron approximation, does not agree with the data, whereas the latter curve fits the I β_{4p} results very well, suggesting the possibility of strong interchannel coupling between the $4d$ photoemission channels and the channels that lead to the "$4p$" peak. Interchannel coupling is plausible if the $4d^8 4f$ state reached via the "$4p$" transition is regarded as a multielectron satellite of the $4d^9$ final state. Identification of the exact mechanism by which these channels can couple through the continuum and lead to a β_{4p} similar to β_{4d} would require a more detailed theoretical model than any presently available.

IV. CONCLUSIONS

Photon-energy-dependent measurements of the behavior of the I $4d$ and "$4p$" subshells in CH_3I have illustrated some important single-electron and multielectron effects. The I $4d$ cross section and asymmetry parameter show pronounced changes under the influence of a shape resonance and a Cooper minimum in the $4d \rightarrow \epsilon f$ outgoing photoelectron channel. Analogous results have been observed for the Xe $4d$ subshell,[7] indicating not only the atomiclike nature of the I atom in CH_3I, but yielding useful information about the Z dependence of these one-electron effects on $4d$-subshell ionization.

The first measurements as a function of photon energy for a "$4p$" subshell in the interesting elemental series Te-Ba have shown that interchannel coupling with the $4d$ channel strongly perturbs the "$4p$" asymmetry parameter. Still to be understood is the nature and relative composition of the final states other than $4d^8 4f$ contributing to the I "$4p$" peak, and how these states couple to the I $4d$ manifold to cause β_{4p} to be similar to β_{4d}. Further experimental studies on "$4p$" subshells in this region of the Periodic Table, especially $Z=54$ (Xe), are needed to aid in this understanding.

ACKNOWLEDGMENTS

This work was supported by the Director, Office of Energy Research, Office of Basic Energy Sciences, Chemical Sciences Division of the U.S. Department of Energy under Contract No. DE-AC03-76SF00098. It was performed at the Stanford Synchrotron Radiation Laboratory, which is supported by the U.S. Department of Energy (Office of Basic Energy Sciences) and the National Science Foundation (Division of Materials Research). One of us (U.B.) would like to acknowledge support by the Deutsche Forschungsgemeinschaft and another (H.G.K.) would like to acknowledge support by a Wigner fellowship.

*Present address: Department of Chemistry, Pennsylvania State University, University Park, PA 16802.

†Present address: Research and Development Division, Corning Glass Works, Corning, NY 14831.

‡Permanent address: Fachbereich Physik, Technische Universität Berlin, D-1000 Berlin 12, West Germany.

[1]S. Svensson, N. Mårtennson, E. Basilier, P. Å. Malmquist, U. Gelius, and K. Siegbahn, Phys. Scr. **14**, 141 (1976).

[2]J. B. West, P. R. Woodruff, K. Codling, and R. G. Houlgate, J. Phys. B **9**, 407 (1976).

[3]L. Torop, J. Morton, and J. B. West, J. Phys. B **9**, 2035 (1976).

[4]S. P. Shannon, K. Codling, and J. B. West, J. Phys. B **10**, 825 (1977).

[5]M. S. Banna, M. O. Krause, and F. Wuilleumier, J. Phys. B **12**, L125 (1979).

[6]M. O. Krause, T. A. Carlson, and P. R. Woodruff, Phys. Rev. A **24**, 1374 (1981).

[7]S. H. Southworth, P. H. Kobrin, C. M. Truesdale, D. Lindle, S. Owaki, and D. A. Shirley, Phys. Rev. A **24**, 2257 (1981).

[8]S. Southworth, U. Becker, C. M. Truesdale, P. H. Kobrin, D. W. Lindle, S. Owaki, and D. A. Shirley, Phys. Rev. A **28**, 261 (1983).

[9]J. W. Cooper, Phys. Rev. Lett. **13**, 762 (1964).

[10]S. T. Manson and D. J. Kennedy, Chem. Phys. Lett. **7**, 387 (1970).

[11]S. T. Manson, Phys. Rev. Lett. **26**, 219 (1971).

[12]D. J. Kennedy and S. T. Manson, Phys. Rev. A **5**, 227 (1972).

[13]G. Wendin, J. Phys. B **6**, 42 (1973).

[14]M. Y. Amusia, N. B. Berezina, and L. V. Chernysheva, Phys. Lett. **51A**, 101 (1975).

[15]M. Y. Amusia and V. K. Ivanov, Phys. Lett. **59A**, 194 (1976).

[16]G. Wendin and M. Ohno, Phys. Scr. **14**, 148 (1976).

[17]W. R. Johnson and V. Radojević, J. Phys. B **11**, L773 (1978).
[18]M. Y. Amusia, Comments At. Mol. Phys. **8**, 61 (1979).
[19]W. Ong and S. T. Manson, Phys. Rev. A **21**, 842 (1980).
[20]K.-N. Huang, W. R. Johnson, and K. T. Cheng, At. Data Nucl. Data Tables **26**, 33 (1981).
[21]M. G. White, R. A. Rosenberg, G. Gabor, E. D. Poliakoff, G. Thornton, S. Southworth, and D. A. Shirley, Rev. Sci. Instrum. **50**, 1288 (1979).
[22]C. N. Yang, Phys. Rev. **74**, 764 (1948).
[23]S. Southworth, C. M. Truesdale, P. H. Kobrin, D. W. Lindle, W. D. Brewer, and D. A. Shirley, J. Chem. Phys. **76**, 143 (1982).
[24]F. Wuilleumier and M. O. Krause, J. Electron Spectrosc. Relat. Phenom. **15**, 15 (1979).
[25]G. O'Sullivan, J. Phys. B **15**, L327 (1982).
[26]S. T. Manson and J. W. Cooper, Phys. Rev. **165**, 126 (1968).
[27]J. W. Cooper, Phys. Rev. **128**, 681 (1962).
[28]R. Haensel, G. Keitel, P. Schreiber, and C. Kunz, Phys. Rev. **188**, 1375 (1969).
[29]D. L. Ederer and M. Manalis, J. Opt. Soc. Am. **65**, 634 (1975).
[30]A. P. Lukirskii, I. A. Brytov, and T. M. Zimkina, Opt. Spektrosk. **17**, 438 (1964) [Opt. Spectrosc. **17**, 234 (1964)].
[31]D. L. Ederer, Phys. Rev. Lett. **13**, 760 (1964).
[32]T. M. Zimkina and S. A. Gribovskii, J. Phys. (Paris) Colloq. **10**, C4-282 (1971).
[33]J. P. Connerade, Proc. R. Soc. London, Ser. A **347**, 581 (1976).
[34]For $Z=56$ (Ba), the $4f$ orbital has less continuum character, and very strong intershell-correlation effects related to the shape-resonance effects for lighter elements (e.g., Xe and I) are important. For discussions of both types of effects and their intimate relationship, see G. Wendin, J. Phys. B **9**, L297 (1976); J. P. Connerade, Contemp. Phys. **19**, 415 (1978); K. T. Cheng and C. Froese Fischer, Phys. Rev. A **28**, 2811 (1983); K. T. Cheng and W. R. Johnson, *ibid.* **28**, 2820 (1983) and references therein.
[35]T. Tuomi, B. Sonntag, and G. Zimmerer, Deutsche Elektronen-Synchrotron (Hamburg) Report No. SR-72/14 (1972) (unpublished).
[36]F. J. Comes, U. Nielsen, and W. H. E. Schwarz, J. Chem. Phys. **58**, 2230 (1973).
[37]F. C. Brown, C. Gahwiller, H. Fujita, A. B. Kunz, W. Schiefley, and N. Carrera, Phys. Rev. B **2**, 2126 (1970).
[38]P. K. Carroll, E. T. Kennedy, and G. O'Sullivan, Appl. Opt. **19**, 1454 (1980).
[39]M. Pettini, M. Mazzoni, and G. P. Tozzi, Phys. Lett. **82A**, 168 (1981).
[40]M. Cardona, R. Haensel, D. W. Lynch, and B. Sonntag, Phys. Rev. B **2**, 1117 (1970).
[41]H. Petersen, K. Radler, B. Sonntag, and R. Haensel, J. Phys. B **8**, 31 (1975).
[42]K. Radler and B. Sonntag, Chem. Phys. Lett. **39**, 371 (1976).
[43]A. P. Hitchcock and C. E. Brion, J. Electron Spectrosc. Relat. Phenom. **13**, 193 (1978).
[44]J. Cooper and R. N. Zare, J. Chem. Phys. **48**, 942 (1968).
[45]P. H. Kobrin, P. A. Heimann, H. G. Kerkhoff, D. W. Lindle, C. M. Truesdale, T. A. Ferrett, U. Becker, and D. A. Shirley, Phys. Rev. A **27**, 3031 (1983).